

Published in final edited form as:

*Biomaterials*. 2014 July ; 35(22): 5921–5931. doi:10.1016/j.biomaterials.2014.03.073.

## Tissue-engineered cartilage with inducible and tunable immunomodulatory properties

Katherine A. Glass<sup>1,2</sup>, Jarrett M. Link<sup>1,2</sup>, Jonathan M. Brunger<sup>1,2</sup>, Franklin T. Moutos<sup>1</sup>, Charles A. Gersbach<sup>1,2,\*</sup>, and Farshid Guilak<sup>1,2,3,\*</sup>

<sup>1</sup>Department of Orthopaedic Surgery, Duke University Medical Center, Durham, NC 27710

<sup>2</sup>Department of Biomedical Engineering, Duke University, Durham, NC 27708

<sup>3</sup>Department of Cell Biology, Duke University Medical Center, Durham, NC 27710

### Abstract

The pathogenesis of osteoarthritis is mediated in part by inflammatory cytokines including interleukin-1 (IL-1), which promote degradation of articular cartilage and prevent human mesenchymal stem cell (MSC) chondrogenesis. In this study, we combined gene therapy and functional tissue engineering to develop engineered cartilage with immunomodulatory properties that allow chondrogenesis in the presence of pathologic levels of IL-1 by inducing overexpression of IL-1 receptor antagonist (IL-1Ra) in MSCs via scaffold-mediated lentiviral gene delivery. A doxycycline-inducible vector was used to transduce MSCs in monolayer or within 3D woven PCL scaffolds to enable tunable IL-1Ra production. In the presence of IL-1, IL-1Ra-expressing engineered cartilage produced cartilage-specific extracellular matrix, while resisting IL-1-induced upregulation of matrix metalloproteinases and maintaining mechanical properties similar to native articular cartilage. The ability of functional engineered cartilage to deliver tunable anti-inflammatory cytokines to the joint may enhance the long-term success of therapies for cartilage injuries or osteoarthritis.

### Keywords

bioactive biomaterial; mesenchymal stem cell; lentivirus; cartilage repair; osteoarthritis; immunomodulation; immunoengineering

---

© 2014 Elsevier Ltd. All rights reserved.

Correspondence address: Farshid Guilak, Ph.D., Duke University Medical Center, 375 MSRB, Box 3093, Durham, NC 27710 USA, Phone (919) 684-2521, Fax (919) 681-8490, [guilak@duke.edu](mailto:guilak@duke.edu). Charles A. Gersbach, Ph.D., Department of Biomedical Engineering, Room 136 Hudson Hall, Box 90281, Duke University, Durham, NC 27708-0281, Phone: 919-613-2147, Fax: 919-668-0795, [charles.gersbach@duke.edu](mailto:charles.gersbach@duke.edu).

\*These authors contributed equally.

#### Author Contributions:

K.A.G., C.A.G., and F.G. developed the concept and designed the experiments. K.A.G. and J.M.L. performed experiments and collected and analyzed the data. J.M.B. and F.T.M. provided technical support and conceptual advice. K.G. wrote the manuscript. All authors edited the manuscript.

**Publisher's Disclaimer:** This is a PDF file of an unedited manuscript that has been accepted for publication. As a service to our customers we are providing this early version of the manuscript. The manuscript will undergo copy editing, typesetting, and review of the resulting proof before it is published in its final citable form. Please note that during the production process errors may be discovered which could affect the content, and all legal disclaimers that apply to the journal pertain.

## Introduction

Arthritis is the leading cause of disability in the United States and affects an estimated 50 million people, with over half of these patients suffering from osteoarthritis (OA) [1]. Risk factors for OA include age, obesity, altered biomechanics, and joint injury, including focal articular cartilage defects [2, 3]. The progressive cartilage degeneration that occurs with OA frequently progresses such that total joint replacement is required, as there are currently no disease-modifying treatments [2]. Because articular cartilage lacks a natural ability to self-repair, tissue engineering strategies may provide solutions for both the repair of focal cartilage defects and the more extensive cartilage degeneration in OA [4, 5]. Typically, engineered cartilage constructs are either grown *in vitro* and implanted or formed *in situ* from a combination of cells, biomaterials, and bioactive stimuli [4, 6]. We have previously shown that a three-dimensionally (3D) woven, porous, biomimetic scaffold made from poly( $\epsilon$ -caprolactone) (PCL) mimics the nonlinear, anisotropic, compressive, and inhomogeneous mechanical properties of articular cartilage and supports chondrogenesis and extracellular matrix deposition by human mesenchymal stem cells (MSCs) [7–9]. Despite major advances in the control of biomechanical and biochemical properties of engineered tissues, there remains a lack of clinical success with engineered cartilage replacements [5].

One challenge in the ultimate clinical success of these technologies is the potential detrimental influence of the inflammatory environment of the diseased joint [10]. The pathogenesis of OA and post-traumatic arthritis following joint injury is mediated in part by the action of pro-inflammatory cytokines such as interleukin-1 (IL-1), which are found at elevated concentrations in the synovial fluid of OA joints [11–13]. IL-1 promotes catabolic and anti-anabolic signaling in articular chondrocytes by inducing release of other pro-inflammatory factors such as matrix metalloproteinases (MMPs) and nitric oxide (NO) and down-regulating gene expression of primary extracellular matrix (ECM) components including type II collagen and aggrecan [11, 12]. IL-1 has been shown to inhibit integrative repair of the meniscus *in vitro* by upregulating MMPs and decreasing cellular proliferation [14–16]. More recent *in vitro* evidence shows that IL-1 also prevents MSC chondrogenesis and matrix accumulation in pellet culture [17, 18] and within biomaterial scaffolds [19, 20]. In this regard, *in vivo* implantation of MSCs for articular cartilage repair can be associated with a loss of chondrogenic potential as well as a shift toward a more hypertrophic phenotype, which may result in endochondral ossification of the implant [21, 22]. There is growing evidence that the inflammatory environment within the joint may be in part responsible for this altered MSC differentiation [21, 23, 24]. Thus, inflammatory signaling mediated by IL-1 within the OA or injured joint may inhibit the development and homeostasis of tissue-engineered cartilage while continuing to advance the degradation of the native tissue.

IL-1 receptor antagonist (IL-1Ra) is a natural inhibitor of IL-1 that competes with IL-1 in binding to the IL-1 receptor [25]. Daily systemic injection of recombinant human IL-1Ra (anakinra) is approved for treatment of rheumatoid arthritis and has been explored in OA treatment, but its efficacy is limited by its short half-life of only a few hours [26]. Intra-articular gene delivery of IL-1Ra, or delivery of cells which have been transduced *ex vivo*,

has been studied extensively in animal models and has progressed to clinical trials (reviewed in [27]). To date, IL-1Ra gene therapy strategies for OA have employed constitutive expression cassettes, which lack regulation of transgene expression. Since IL-1-mediated inflammation may be necessary for early stages of tissue repair such as bone remodeling during fracture healing [28, 29], the ability to directly regulate transgene expression could be of great value in the controlled delivery of anti-cytokine therapies. Advances in doxycycline (dox)-inducible expression systems [30, 31] that facilitate tunable control of transgene expression via oral administration of a chemical inducer have yet to be explored for the regulation of OA gene therapy.

Previous approaches for IL-1Ra gene therapy [27, 32–34] have been designed to protect joints from further arthritic degeneration, but are not designed to provide a functional replacement for severely damaged cartilage, which may limit their efficacy in OA treatment. Additionally, injection of virus directly into the joint does not provide control over which cell types are transduced, and it has been shown that most of the transduction occurs in the synovium rather than in articular cartilage [32], although recent studies have shown that AAV-based transduction of native chondrocytes is possible [35, 36]. Biomaterial-mediated gene delivery from a tissue-engineering scaffold may address these shortcomings by providing spatially-defined control of cell transduction *in situ* and localizing production of the therapeutic protein to the engineered repair tissues. We recently established a technique using poly-L-lysine (PLL) to immobilize lentivirus (LV) encoding constitutively expressed morphogenetic transgenes to a 3D woven PCL scaffold [37]. MSCs seeded onto these scaffolds were efficiently engineered to express these transgenes, leading to robust chondrogenic differentiation without the need to supplement cultures with exogenous growth factors. Scaffold-mediated transduction with LV enables spatially-defined and sustained transgene expression that may potentially direct tissue development *in vivo*. The ability to inhibit the catabolic effects of IL-1 on engineered cartilage while maintaining structural and functional properties that match native cartilage may enhance the long-term success of tissue engineering approaches to cartilage repair.

The goal of this study was to combine a gene therapy approach for inducible and tunable anti-cytokine therapy with functional cartilage tissue engineering to create a cartilage construct capable of supporting chondrogenesis in the presence of the catabolic mediator IL-1. We employed scaffold-mediated LV gene delivery of a dox-inducible IL-1Ra expression vector to MSCs to engineer cartilage constructs with tunable IL-1Ra overexpression. We investigated the magnitude and duration of MSC overexpression of IL-1Ra in monolayer cultures as well as in developing cartilage constructs. Furthermore, we characterized the ability of IL-1Ra-expressing constructs to inhibit the detrimental effects of IL-1 on the development of *in vitro* engineered cartilage by analyzing histology, biochemical composition, release of inflammatory factors, and mechanical properties.

## Materials and Methods

### Lentivirus production

The dox-inducible lentiviral vector (TMPrtTA, provided by the Danos Lab) is a single “tet-on” vector that constitutively co-expresses an improved reverse tetracycline-controlled

transcriptional activator [30, 31, 38]. The dox-inducible vector was modified to include an IRES-puromycin expression cassette. IL-1Ra and enhanced green fluorescence protein (eGFP) coding sequences were cloned into the modified TMPrtTA vector [30] or a constitutive lentiviral vector with the EF-1 $\alpha$  promoter (Addgene 12250) [39] (Fig. 1A). HEK293T/17 (ATCC CRL-11268, Manassas, VA) were co-transfected with the appropriate expression transfer vector (20  $\mu$ g), packaging plasmid (psPAX2, Addgene 12259, 15  $\mu$ g), and envelope plasmid (pMD2.G, Addgene 12260, 6  $\mu$ g) via calcium phosphate precipitation to produce VSV-G pseudotyped LV as previously described [40]. LV was concentrated ~80 fold via centrifugation in 100 kDa MWCO filters (Millipore, Cork, Ireland) and frozen at  $-80^{\circ}\text{C}$ . Biological titration of eGFP LV was performed in HeLa (ATCC CCL-2, Manassas, VA) using the Accuri flow cytometer (BD Biosciences, Franklin Lakes, NJ), to obtain the functional titer in transducing units/mL as previously described [40].

### MSC isolation and expansion

MSCs were isolated from human bone marrow waste from three adult bone marrow transplant donors at Duke University Medical Center. Non-adherent cells were removed by the end of the first passage. MSCs from each donor were combined in equal numbers into a superlot and expanded for 4 passages prior to use in experiments. Expansion medium consisted of DMEM-LG (Gibco, Life Technologies, Carlsbad, CA), 10% lot-selected FBS (Hyclone, Thermo Scientific, Waltham, MA), 1% pen/strep (Gibco), and 10 ng/mL basic fibroblast growth factor (bFGF) (Roche, Basel, Switzerland).

### LV transduction and optimization of doxycycline concentration in monolayer culture

MSCs were plated on tissue culture plastic 1 day prior to transduction (100 cells/ $\text{mm}^2$ ). For transduction, MSC culture medium was replaced with concentrated constitutive or inducible IL-1Ra LV that was resuspended in MSC expansion medium to a final biological titer of  $7.6 \times 10^5$  transducing units / mL with 4  $\mu\text{g}/\text{mL}$  polybrene (Sigma-Aldrich, St. Louis, MO). Medium was replaced after 16 hours, and this day was defined as day 0. Control MSCs were not transduced. MSCs were treated with various concentrations of dox (Sigma-Aldrich). Conditioned medium was collected and frozen at  $-20^{\circ}\text{C}$  and replaced every 3 days. MSCs were passaged into new wells every 6 days at the same density as initial plating and cultured for 30 days following transduction. Conditioned medium was assayed for IL-1Ra production via human IL-1Ra ELISA, according to the manufacturer's protocol (R&D Systems, Cat. No. DY280).

### 3D woven PCL scaffold production

Scaffolds were woven from multifilament PCL yarns (EMS-Griltech, Domat, Switzerland) using a custom-built weaving machine, as previously described [7]. For this study, 7 layers of yarns were axially oriented in alternating x and y directions with a third set of fibers passing through the thickness of the structure (z-direction). Total void space within the scaffold was ~61% with interconnected rectangular pores measuring approximately  $350 \mu\text{m} \times 250 \mu\text{m} \times 100 \mu\text{m}$ . Scaffolds were treated with 4N NaOH for 16 hours to increase surface hydrophilicity, rinsed in DI H<sub>2</sub>O, and dried. Scaffolds were subsequently heat set for 10 min at  $57^{\circ}\text{C}$  in DI H<sub>2</sub>O. Dried scaffolds were then punched using a trephine to obtain uniform 5 mm disks. For scanning electron microscopy, disks were mounted, sputter-coated with gold,

and imaged with a scanning electron microscope (FEI XL30 SEM-FEG, Eindhoven, Netherlands). For tissue engineering experiments, disks were ethylene-oxide sterilized in 24 well ultra-low attachment plates (Corning, Corning, NY) prior to use.

### **MSC transduction via immobilization of LV on 3D woven PCL scaffolds**

Scaffold disks were incubated with 0.002% PLL (Sigma-Aldrich) overnight to facilitate non-covalent association of viral particles with the scaffold surface through charge interaction between the positively charged PLL and negatively charged LV [37, 41, 42]. Scaffolds were then rinsed in PBS (Gibco) and incubated with concentrated LV for 1.5 hours, rinsed again, and seeded with 465K MSCs ( $16.7 \times 10^6$  cells/mL) at the end of passage 4 [37]. The biological titer of concentrated LV for all scaffold-mediated transduction experiments was measured as  $1.6 \times 10^7$  transducing units/mL. MSCs were also seeded directly onto rinsed, PLL-coated scaffolds to produce non-transduced (NT) MSC constructs. One hour after seeding, expansion medium was added to each sample.

### **Transgene expression analysis of transduced MSCs in engineered cartilage constructs**

To evaluate transduction efficiency during scaffold-mediated transduction, MSCs were seeded and transduced as above with either constitutive or inducible eGFP LV (n=3) or remained non-transduced (n=2). Two days following transduction, all constructs were given 1  $\mu\text{g/mL}$  dox. Six days after transduction, constructs were digested in Pronase (Calbiochem, San Diego, CA) and Collagenase type II (Worthington, Lakewood, NJ) and minced to isolate MSCs for flow cytometry, as previously described [37].

To assess the extent to which IL-1Ra production with the dox-inducible vector was tunable and repeatable during development of engineered cartilage constructs, MSCs were seeded and transduced as described above with inducible IL-1Ra LV or inducible eGFP LV. After 11 days of pre-culture in expansion medium to allow the seeded cells to proliferate and fill the pores within the scaffold, constructs were switched to chondrogenic medium for 36 days and subjected to different treatment courses of 1  $\mu\text{g/mL}$  dox (n=4/group). Chondrogenic medium consisted of DMEM-HG (Gibco), 1% pen/strep (Gibco), 1% ITS<sup>+</sup>, 100 nM dexamethasone (Sigma-Aldrich), 50  $\mu\text{g/mL}$  L-ascorbic acid (Sigma-Aldrich), 40  $\mu\text{g/mL}$  L-proline (Sigma-Aldrich), and 10 ng/mL rhTGF- $\beta$ 3 (R&D Systems, Minneapolis, MN). Medium was collected and replaced every 3 days.

### **In vitro inflammatory challenge during development of engineered cartilage constructs**

MSCs were transduced and seeded as described above, onto scaffolds with either immobilized inducible IL-1Ra LV, inducible eGFP LV, or without LV. Some constructs were harvested immediately after addition of expansion medium and frozen at  $-20^\circ\text{C}$  for biochemical and biomechanical analyses (Day -11, n=5/group). MSCs were allowed to proliferate in expansion medium for 11 days, and constructs were harvested immediately prior to chondrogenic induction and frozen at  $-20^\circ\text{C}$  (Day 0, n=5/group). Dox (1  $\mu\text{g/mL}$ ) was added to medium for all samples starting 3 days prior to chondrogenic induction. Beginning 3 days after chondrogenic induction (Day 3), constructs were either treated with 0.1 or 1 ng/mL rhIL-1 $\alpha$  (R&D Systems) or left untreated (n=7/group). Half of the conditioned culture medium for each sample was collected, frozen at  $-20^\circ\text{C}$ , and replaced

every 3 days (n=5) to measure secretion of IL-1Ra, inflammatory mediators, and glycosaminoglycans (GAGs). After 27 days of chondrogenesis, samples were either frozen at  $-20^{\circ}\text{C}$  (n=5/group) or fixed for histological processing (n=2/group) to be evaluated for production of cartilage-specific ECM and mechanical properties.

## Histology

Constructs were fixed in 4% paraformaldehyde with 100 mM sodium cacodylate overnight. Subsequently, constructs were dehydrated through a series of ethanol washes, cleared in xylenes, embedded in paraffin, and sectioned at 8  $\mu\text{m}$  per section. Sections from each sample were stained for GAGs with 0.1% aqueous Safranin-O, collagen with 0.02% aqueous fast green, and stained for cell nuclei with hematoxylin. Immunohistochemistry was performed with monoclonal antibodies to type I collagen (ab90395; Abcam, Cambridge, MA), type II collagen (II-II6B3; Developmental Studies Hybridoma Bank, University of Iowa, Iowa City, IA), or type X collagen (C7974; Sigma-Aldrich). For all IHC, slides with sections of each sample were cleared, rehydrated, and digested with pepsin for epitope retrieval (Digest-All, Invitrogen). After probing with appropriate primary antibodies, all samples were probed with the same biotinylated anti-mouse secondary antibody (ab97021; Abcam), treated with HRP conjugate (Invitrogen), and finally incubated with chromagenaminoethylcarbazole (AEC) single solution (Invitrogen). Human osteochondral plugs were used as positive controls for each antibody and for the general histological stain. Negative controls without primary antibody were also prepared for each slide.

## Biochemical and mechanical analyses

Constructs (n=5/group) were thawed from  $-20^{\circ}\text{C}$  and a core was harvested from the center of the construct using a trephine to create a uniformly sized 3 mm sample for biomechanical analyses. Compression testing was performed using the ELF 3100 series (Bose, Framingham, MA). Unconfined testing was performed by applying sequential strains of 4, 8, and 12% to the constructs in a PBS bath after equilibration of a 4 gf tare load. At each strain step, constructs were allowed to equilibrate for 900 seconds and  $E_Y$  was calculated as the slope of a linear regression of the equilibrium stress-strain plot. Confined compression testing was performed by press-fitting the sample into a cylindrical chamber of the same diameter and applying force with a piston onto a rigid porous platen (porosity of 50%, pore size of 50–100  $\mu\text{m}$ ). Following equilibration of a 10 gf tare load, a step 30 gf load was applied and samples were allowed to creep to equilibrium over 800 seconds, and  $H_A$  was determined [43].

The annulus of each construct was lyophilized and digested in papain buffer (125 mg/mL papain (Sigma-Aldrich), 100 mM phosphate buffer, 10mM cysteine, and 10mM EDTA, pH 6.3) overnight at  $60^{\circ}\text{C}$  for biochemical analyses. The Quant-iT™ PicoGreen® dsDNA Assay Kit (Invitrogen) was used to measure dsDNA content, according to manufacturer's instructions. GAG content was assessed with the dimethylmethylene blue (DMMB) assay, using chondroitin sulfate A from bovine trachea (Sigma-Aldrich) as a standard, and reading the plate at 525 nm [44]. Collagen content in each sample was determined via the orthohydroxyproline assay, using trans-4-hydroxyproline-L (Sigma) as a standard (with 1  $\mu\text{g}$  of OHP equivalent to 7.46  $\mu\text{g}$  collagen), and reading the plate at 540 nm [45].



## Culture Media Analyses

Human IL-1Ra ELISA (R&D Systems, Cat. No. DY280) was performed for all quantifications of IL-1Ra secretion into culture media, following the manufacturer's protocol. Human PGE<sub>2</sub> secretion was also quantified via ELISA (R&D Systems, Cat. No. SKGE004B). Total specific MMP activity was assayed by measuring quenching of a fluorescent substrate (Dab-Gly- Pro-Leu-Gly-Met-Arg-Gly-Lys-Flu, Sigma-Aldrich) as the substrate is cleaved mostly by MMP-13, but also by MMP-1,-2,-3, and -9 in the sample culture media [14]. The total specific MMP activity in each sample is measured as the difference in fluorescence between replicates incubated with a broad-spectrum MMP inhibitor, GM6001 (EMD Biosciences Inc, San Diego, CA), and a scrambled negative control peptide (EMD Biosciences Inc). Values for all samples were above those of unconditioned culture media. GAG release in the culture media was assayed with the DMMB assay mentioned above, with the standards prepared in culture media rather than in papain.

## Statistical analysis

For all assays, the lower limit of detection was calculated conservatively as the average of the blank replicates plus two standard deviations. All assays were run in duplicate. Two-factor ANOVA with Fisher's LSD post-hoc and  $\alpha=0.05$ , performed with SPSS Statistics software was used in all statistical analyses.

## Results

### Tunable IL-1Ra secretion in MSCs

We first examined the dynamic range of inducible and IL-1Ra production in MSCs transduced in monolayer culture, and compared it to constitutive IL-1Ra production. Following treatment with concentrations of dox ranging from 0 to 10  $\mu\text{g/mL}$ , transduced MSCs produced tunable levels of IL-1Ra peaking 2–3 orders of magnitude above the baseline in the absence of dox (Fig. 1B). Non-transduced (NT) MSCs did not produce detectable levels of IL-1Ra, whereas transduced cells produced approximately 1 ng/mL IL-1Ra in the absence of dox, indicative of low levels of leaky IL-1Ra expression. IL-1Ra secretion was measured for up to 27 days in MSCs transduced with the constitutive or inducible vector and cultured with dox doses of 0, 0.1, or 1  $\mu\text{g/mL}$  (Fig. 1C). MSCs transduced with the inducible vector and treated with 1  $\mu\text{g/mL}$  of dox produced significantly higher levels of IL-1Ra than all other conditions for the duration of the experiment (~100–1000 ng/mL IL-1Ra,  $p<0.05$  at all time points), and thus this vector and dox dose was used for all subsequent tissue engineering experiments.

### Scaffold-mediated transduction of MSCs produces robust and tunable transgene expression

Next, we determined the efficiency of scaffold-mediated transduction of inducible or constitutive eGFP LV six days following seeding of MSCs on 3D woven PCL scaffolds [8] (Fig. 2A). MSCs were seeded and transduced uniformly across the scaffold as visualized by fluorescence imaging of eGFP+ cells infiltrating pores in the woven structure and between

the fibers in a bundle (Figs. 2B& 2C). The percentage of eGFP<sup>+</sup> cells was determined by flow cytometry following enzymatic isolation of the cells from the constructs (Fig. S1). The percentages of eGFP<sup>+</sup> MSCs in the constitutive and inducible eGFP-expressing constructs were 89.8% and 84.5%, respectively (Fig. 2D).

We then sought to develop an engineered cartilage construct capable of producing IL-1Ra at therapeutic concentrations, i.e. ~2–3 orders of magnitude higher than pathophysiologic IL-1 levels [13, 46], under dox-inducible control. To investigate the dynamics of IL-1Ra expression during development of cartilage tissue constructs following scaffold-mediated transduction, we prepared inducible IL-1Ra-expressing or eGFP-expressing constructs and monitored transgene expression during 36 days of chondrogenesis with different treatment courses of 1 µg/mL dox: (1) constant treatment, (2) intermittent treatment alternating every nine days, or (3) no treatment. Dox-induced IL-1Ra production exceeded 100 ng/mL for 36 days of culture with constant dox induction and was reproducibly switched on and off with dox addition or removal (Fig. 2E). Baseline levels in the absence of dox ranged from 0.3 – 3 ng/mL IL-1Ra over the course of the experiment. IL-1Ra production decreased gradually to baseline over the nine-day periods of dox withdrawal. Upon re-introduction of dox, IL-1Ra production increased rapidly to levels matching the group receiving constant dox treatment.

### Enhanced GAG production by IL-1Ra-expressing constructs in inflammatory conditions

We next explored the ability of the inducible IL-1Ra-expressing constructs to undergo chondrogenesis during an *in vitro* inflammatory challenge with pathophysiologic levels of IL-1 $\alpha$ . Three days after chondrogenic induction, constructs transduced with no LV, eGFP LV, or IL-1Ra LV were treated with 0.1 or 1 ng/mL IL-1 $\alpha$  for the duration of the study or left untreated. IL-1Ra secretion was not affected by addition of IL-1 to culture media and exceeded 100 ng/mL for 27 days in chondrogenic culture conditions (Fig. S2). NT and eGFP-expressing constructs did not produce detectable levels of IL-1Ra in any media condition. DNA content in the engineered cartilage constructs approximately tripled during the expansion phase and subsequently doubled during chondrogenesis (Fig. S3).

GAG deposition normalized to DNA content (GAG/DNA) in constructs without IL-1 treatment was similar for all three groups (NT, eGFP, IL-1Ra) at 40 µg/µg at day 27 (Fig. 3A). IL-1 treatment significantly reduced GAG/DNA deposition in NT and eGFP-expressing constructs, to ~7.3 µg/µg with 0.1 ng/mL IL-1 and ~5.5 µg/µg with 1 ng/mL IL-1 ( $p < 0.05$ ). However, IL-1Ra-expressing constructs contained significantly higher GAG/DNA than NT or eGFP-expressing constructs when cultured in the presence of IL-1 at either 0.1 ng/mL (~32.5 µg/µg) or 1 ng/mL (~15.4 µg/µg) ( $p < 0.05$ ), demonstrating the ability of the IL-1Ra-expressing constructs to antagonize IL-1 signaling in a dose-dependent manner. Similar results were seen for total GAG content per construct without normalizing to DNA (Fig. S4). Safranin-O red staining for GAG in histological sections also showed robust GAG production in untreated constructs (Fig. 3B). In both IL-1 treatment groups, there was very little GAG staining present in the NT and eGFP-expressing constructs. IL-1Ra-expressing constructs maintained rich GAG staining at 0.1 ng/mL IL-1 and reduced staining was observed at 1 ng/mL IL-1, corroborating the quantitative biochemical results that show



IL-1Ra overexpression markedly improves GAG deposition in engineered cartilage constructs exposed to IL-1.

### Enhanced collagen production in IL-1Ra-expressing constructs in inflammatory conditions

In the absence of IL-1, engineered cartilage constructs harvested at day 27 accumulated total collagen normalized to DNA (collagen/DNA) of ~50  $\mu\text{g}/\mu\text{g}$  (Fig. 4A). Collagen was not detectable at seeding or at the time of chondrogenic induction. Treatment with IL-1 significantly reduced collagen deposition in NT and eGFP-expressing constructs by ~2-fold ( $p < 0.05$ ), with similar levels observed at both doses of IL-1. IL-1Ra-expressing constructs were protected from IL-1-mediated reduction of collagen content, showing similar total collagen deposition to that of constructs in the absence of IL-1. Similar trends were observed for total collagen content per construct without normalizing to DNA (Fig. S5). Furthermore, immunohistochemistry (IHC) was performed to examine the deposition of cartilage-specific types of collagen. Type II collagen is the most abundant collagen found in articular cartilage, and IHC revealed strong type II collagen staining in untreated constructs, which was maintained in IL-1Ra-expressing constructs treated with IL-1 (Fig. 4B). Type I collagen staining was strong in constructs not treated with IL-1, but was greatly reduced in NT and eGFP-expressing constructs treated with IL-1 at either dose (Fig. 4C). A slight reduction in type I collagen staining intensity was observed in IL-1Ra-expressing constructs treated with IL-1 at either dose. Type X collagen staining was detectable but low in all constructs and levels of this ECM protein did not appear to be affected by IL-1 treatment (Fig. 4D).

### Release of inflammatory mediators in response to IL-1

The release and activity of inflammatory mediators in the conditioned medium from engineered cartilage constructs was quantified at various time points in the course of chondrogenesis. Samples collected at three days post-chondrogenic induction were assayed to determine baseline cell activity before initiation of IL-1 treatment. IL-1 stimulated the NT and eGFP-expressing constructs to secrete MMPs at day 9 through day 27 post-chondrogenic induction (Fig. 5A). The conditioned medium of IL-1Ra-expressing constructs treated with 0.1 ng/mL IL-1 showed similar MMP activity to that of constructs cultured without IL-1 at days 9, 18, and 27. IL-1Ra-expressing constructs demonstrated significantly less MMP activity than the other two groups at 1 ng/mL IL-1 at days 9 and 18 ( $p < 0.05$ ), with a trend toward reduced MMP activity at day 27.

We measured levels of the inflammatory mediator prostaglandin E<sub>2</sub> (PGE<sub>2</sub>) because PGE<sub>2</sub> is upregulated in articular cartilage in response to cytokines such as IL-1 or tumor necrosis factor (TNF) [11] and is implicated in the immunomodulatory abilities of undifferentiated MSCs [47, 48]. During chondrogenesis, MSCs in engineered cartilage constructs produced PGE<sub>2</sub> at physiologically relevant concentrations [49] by day 9 (Fig. 5B). IL-1 treatment inhibited PGE<sub>2</sub> secretion in NT and eGFP-expressing constructs at days 9, 18, and 27, with undetectable levels at days 18 and 27 at both IL-1 doses. IL-1Ra-expressing constructs treated with 0.1 ng/mL IL-1 showed significantly higher PGE<sub>2</sub> levels than NT and eGFP-expressing constructs at days 9, 18, and 27 ( $p < 0.05$ ), although levels remained below those of constructs without IL-1 at days 9 and 27. With 1 ng/mL IL-1 treatment, PGE<sub>2</sub> secretion in

IL-1Ra-expressing constructs was not significantly higher than control constructs except at day 27 ( $p < 0.05$ ).

GAG release into conditioned medium increased over the course of the study in all chondrogenic constructs without IL-1 treatment (Fig. 5C). Through day 18, there were no significant differences in GAG release into the culture media. By day 27, the conditioned medium of constructs cultured without IL-1 contained significantly more GAG than all of the IL-1-treated constructs ( $p < 0.05$ ). However, the IL-1Ra-expressing constructs treated with both IL-1 doses produced significantly more GAG in the media than IL-1-treated NT and eGFP-expressing constructs (~2.1 and 1.7-fold higher, respectively,  $p < 0.05$ ).

### Mechanical properties of engineered cartilage constructs

Unconfined compression testing was performed to obtain the equilibrium Young's modulus ( $E_Y$ ) of samples either one hour following seeding, at the time of chondrogenic induction, or after 27 days of chondrogenesis with or without IL-1.  $E_Y$  averaged approximately 1 MPa in all groups and was not affected by tissue production during chondrogenesis or treatment with IL-1 (Fig. 6A). The aggregate modulus ( $H_A$ ) was determined using a confined compression test, and similar values were observed at seeding, induction, and in all IL-1 treated constructs (Fig. 6B). Untreated constructs at day 27 had a significantly greater  $H_A$  than IL-1-treated constructs ( $p < 0.05$ ).

### Discussion

Using a combined gene therapy and tissue engineering approach based on scaffold-mediated transduction of MSCs, we developed engineered cartilage constructs capable of inducible and tunable IL-1Ra production at therapeutically relevant concentrations, while maintaining mechanical properties mimicking those of native cartilage. These IL-1Ra-expressing constructs were protected from the effects of IL-1 exposure, enabling MSC chondrogenesis and the development of functional engineered cartilage within an inflammatory environment. This approach may provide controlled anti-cytokine delivery to the joint, which can enhance tissue regeneration by MSCs and could potentially inhibit the deleterious effects of IL-1 and other downstream cytokines on the native articular cartilage and other joint tissues following injury or arthritis.

An IL-1Ra concentration of ~3 orders of magnitude greater than the IL-1 $\alpha$  concentration is required for effective inhibition by MSCs *in vitro* in a pellet culture model of chondrogenesis [17]. Therefore we hypothesized that our constructs, which secreted 100 ng/mL IL-1Ra, would be able to fully inhibit IL-1 at the pathophysiologic concentration 0.1 ng/mL and partially inhibit IL-1 at 1 ng/mL. Physiologic levels of IL-1 $\alpha$  induced stronger upregulation of inflammatory mediators and tissue degradation in cartilage and meniscal explants than did similar levels of IL-1 $\beta$  [46]. Although IL-1Ra should inhibit the effects of both of these cytokines, we chose the more stringent test of IL-1 $\alpha$  treatment for the *in vitro* inflammatory challenge because of its increased potency at lower, physiologically relevant, concentrations.

In the presence of IL-1 $\alpha$  at physiologic (0.1 ng/mL) and supraphysiologic concentrations (1 ng/mL), dox-inducible secretion of IL-1Ra protected engineered cartilage constructs from the catabolic and anti-anabolic effects of IL-1 on production and retention of extracellular matrix proteins. While these effects were not completely inhibited, IL-1Ra-expressing constructs exposed to 0.1 ng/mL IL-1 maintained 80% of the levels of GAG/DNA that was present in constructs cultured without IL-1 at Day 27 of chondrogenesis, while control constructs that were not expressing IL-1Ra maintained only 18%. The loss of total collagen/DNA induced by IL-1 was fully protected in IL-1Ra-expressing constructs at either concentration of IL-1. Types I and X collagen are more highly expressed in bone than cartilage, and their expression in native cartilage can indicate a transition to a hypertrophic phenotype. However, types I and X collagen are typically upregulated during chondrogenesis of MSCs [50, 51]. Qualitatively, we did not see an increase in types I or X collagen with IL-1 treatment. Although IL-1 has been implicated in the progression from chondrogenesis to endochondral ossification [21, 22], in this study NT and eGFP-expressing constructs were treated with IL-1 beginning day 3 of chondrogenesis, which likely prevented chondrogenesis in these samples altogether.

NT and eGFP-expressing constructs secreted MMPs in response to IL-1 exposure, similar to native cartilage or meniscus explants [46, 52] or other engineered cartilage constructs [52, 53], which likely contributed to poor matrix accumulation in these samples. At 0.1 ng/mL IL-1, the IL-1-induced increase in MMP activity was fully blocked in IL-1Ra-expressing constructs. However, IL-1Ra-expressing constructs treated with 1 ng/mL IL-1 showed levels of MMP activity similar to NT and eGFP-expressing constructs by day 27, again indicating the IL-1Ra levels were not sufficient to fully block the effects of this higher dose of IL-1. Interestingly, these findings do not correlate with the observation that IL-1Ra-expressing constructs contained similar total collagen content at either dose of IL-1. However, qualitatively, we did see a slight decrease in collagen type II IHC staining and a larger decrease in collagen type I IHC staining in IL-1Ra-expressing constructs at 1 ng/mL IL-1 treatment. Since IL-1Ra-expressing constructs in IL-1 treatment conditions have higher ECM retention than NT and eGFP-expressing constructs, the collagen may be cleaved by MMPs but become entrapped rather than diffusing out of the construct. This cleaved but entrapped collagen may be contributing to overall collagen content measured in the digested samples. This finding may also explain why the IL-1Ra-expressing constructs treated with IL-1 did not maintain similar aggregate modulus to those of constructs without any inflammatory stimulus.

Nonetheless, the compressive properties of the constructs in all culture conditions were within the range measured in native articular cartilage [54, 55]. The Young's Modulus ( $E_Y$ ) was not affected by neotissue growth or the addition of IL-1, allowing constructs to maintain controlled, predefined mechanical properties. This finding indicates that, as intended, the compressive stiffness is dominated by the structure of the 3D woven PCL scaffold, and these properties are maintained throughout the culture duration.

Unlike cartilage explants [46] or chondrocyte-based engineered cartilage constructs [53], our engineered cartilage constructs with differentiating human MSCs expressed PGE<sub>2</sub> during chondrogenesis in the absence of IL-1. This finding is consistent with previous studies that

showed human MSCs expressing PGE<sub>2</sub> during chondrogenesis in pellet culture [56, 57]. In the current study, PGE<sub>2</sub> was undetectable at days 18 and 27 in IL-1 treated control constructs, possibly due to the lack of chondrogenic differentiation in these samples. IL-1Ra-expressing constructs, in contrast, maintained similar PGE<sub>2</sub> levels to those of untreated constructs at 0.1 ng/mL IL-1 and still showed some PGE<sub>2</sub> expression at 1 ng/mL IL-1. PGE<sub>2</sub> is postulated to be pro-anabolic in cartilage despite being upregulated by IL-1 [11, 58], and is also part of the pro-anabolic response of cartilage explants under dynamic compression [59]. PGE<sub>2</sub> is also important for chondrogenic commitment of progenitors during endochondral ossification [60] and contributes to the immunomodulatory properties of undifferentiated MSCs *in vivo* [47, 61]. Engineered cartilage constructs implanted *in vivo* could have a similar effect, as the release of PGE<sub>2</sub> may play an immunomodulatory role within the joint. Alternatively, once the engineered cartilage constructs are implanted without exogenous TGF-β3 stimulation, PGE<sub>2</sub> secretion may be reduced.

Although with 0.1 ng/mL IL-1 treatment we measured ~1000-fold more IL-1Ra than IL-1, we still did not see complete inhibition of IL-1 signaling. These findings suggest that MSCs may potentially be more sensitive to IL-1 than primary chondrocytes, and that an even greater excess of IL-1Ra may be required to fully inhibit IL-1α within the engineered cartilage constructs. Furthermore, since IL-1 treatment was initiated early in construct development, the exogenous IL-1 may diffuse more readily into the construct and have a higher partition coefficient [62] before the ECM is produced, whereas the dense ECM of cartilage explants or established pellet aggregates of differentiated stem cells may reduce the effective concentration of IL-1 within the construct. It may be possible to increase the expression levels of IL-1Ra in this system by increasing LV titer on the scaffold or engineering a stronger promoter.

Alternative strategies using biomaterials to improve IL-1Ra protein delivery that have been previously explored by others include depots of IL-1Ra-elastin-like polypeptide fusions [63], controlled release of IL-1Ra from PLGA microspheres to nucleus pulposus *in vitro* [64], and intra-articular delivery of polymer nanoparticle-IL-1Ra conjugates [65]. These approaches showed some success in preventing IL-1-mediated tissue degradation, but may be limited for long-term applications due to loss of IL-1Ra in the first 10–15 days [64, 65] or reduced bioactivity of fusion proteins [63]. Sustained IL-1Ra protein delivery would still require repeated intra-articular injections to address inflammation in the joint, whereas biomaterial-mediated lentiviral gene delivery allows for long-term, controlled production of IL-1Ra within the joint while also facilitating articular cartilage repair. Small molecules like curcumin [66] and NF-κB inhibitors [67] have also shown promise for inhibiting the catabolic effects of pro-inflammatory cytokines on MSC or iPSC-derived tissue engineered cartilage *in vitro*, and may provide alternative approaches for enhancing chondrogenesis.

Biomaterial-mediated gene delivery has been previously used for various applications using immobilization to biomaterial surfaces to spatially control transduction [68–70] or encapsulation within a biomaterial in order to dynamically release a vector [71–73]. Scaffold-mediated viral delivery enables spatially-defined transduction while also expediting the development of an engineered tissue by removing the monolayer culture transduction and expansion step. However, previous biomaterial-mediated gene delivery

strategies have primarily utilized transient gene expression, either by delivering naked plasmid DNA [72, 73] or by delivering non-integrating viral vectors [70, 71, 74], which have limited the transgene expression to days or months. Controllable expression levels over longer time periods are desired for many applications, including regenerative medicine or treatments for chronic diseases. Building on previous work, we engineered IL-1Ra-producing cartilage constructs by coating 3D woven PCL scaffolds with PLL in order to immobilize the LV of interest to the scaffold immediately prior to MSC seeding [37]. As an integrating vector, LV can drive transgene expression indefinitely. We also showed high transduction efficiencies of 85–90% of MSCs isolated from the scaffold, enabling therapeutic levels of IL-1Ra expression of over 100 ng/mL. While IL-1 plays a major role in OA pathogenesis [11] and in prevention of MSC chondrogenesis [17, 18], other cytokines are likely involved as well [12, 17], and future studies may need to target other immunomodulatory pathways. In this regard, this system could be readily adapted to include additional therapeutic transgenes.

An important advance of this system is that the inducible expression cassette allows control of both magnitude and duration of IL-1Ra expression via dox administration. Recent advances in dox-inducible gene expression systems allow for fine-tuned control of transgene expression with low promoter leakiness and sensitivity to lower levels of dox [30]. Dox does not negatively affect MSC chondrogenesis [75] and has also been clinically tested as a disease-modifying drug for OA [76]. Rather than controlling timing of transduction with release of vectors from encapsulation within a biomaterial, in this study IL-1Ra secretion following transduction is exogenously regulated by dox. The ability to switch off IL-1Ra overexpression in cases where inflammation may play an important physiologic role, such as during fracture healing [28, 29], provides an important means of controlling anti-cytokine therapy.

## Conclusions

This study demonstrates the potential to engineer functional implants for cartilage repair with inducible and tunable immunomodulatory properties using a gene therapy approach. We have shown growth and differentiation of functional engineered cartilage constructs while producing therapeutic levels of IL-1Ra during an *in vitro* inflammatory challenge with IL-1. The scaffold-mediated transduction system and the biomimetic mechanical properties of the 3D woven PCL scaffold provide several potential advantages for enhancing articular cartilage repair. Controlling local production of a therapeutic protein with oral or local administration of a chemical inducer would allow exogenous regulation of dosing without repeated local or systemic injections of high concentrations of biologic drugs. While the efficacy of this approach remains to be tested *in vivo*, the controlled release of immunomodulatory mediators may have therapeutic effects throughout the joint, in addition to a protective effect on the engineered cartilage.

## Supplementary Material

Refer to Web version on PubMed Central for supplementary material.

## Acknowledgments

Supported by NIH grants AR061042, AR50245, AR48852, AG15768, AR48182, AG46927, OD008586, NSF CAREER Award CBET-1151035, the Collaborative Research Center, AO Foundation, Davos, Switzerland, the Arthritis Foundation, the Nancy Taylor Foundation, and the NSF GRFP. We thank Tyler Gibson for modifications to the TMPPrTA vector and Christopher Rowland for assistance with SEM imaging. We also thank Dr. Nelson Chao for providing bonemarrow (NIH grant P01 CA47741).

## References

1. Lawrence RC, Felson DT, Helmick CG, Arnold LM, Choi H, Deyo RA, et al. Estimates of the prevalence of arthritis and other rheumatic conditions in the United States. Part II. *Arthritis Rheum.* 2008; 58(1):26–35. [PubMed: 18163497]
2. Abramson SB, Attur M. Developments in the scientific understanding of osteoarthritis. *Arthritis Res Ther.* 2009; 11(3):227. [PubMed: 19519925]
3. Anderson DD, Chubinskaya S, Guilak F, Martin JA, Oegema TR, Olson SA, et al. Post-traumatic osteoarthritis: improved understanding and opportunities for early intervention. *J Orthop Res.* 2011; 29(6):802–9. [PubMed: 21520254]
4. Chung C, Burdick JA. Engineering cartilage tissue. *Adv Drug Deliv Rev.* 2008; 60(2):243–62. [PubMed: 17976858]
5. Johnstone B, Alini M, Cucchiarini M, Dodge GR, Eglin D, Guilak F, et al. Tissue engineering for articular cartilage repair--the state of the art. *Eur Cell Mater.* 2013; 25:248–67. [PubMed: 23636950]
6. Vacanti JP, Langer R. Tissue engineering: the design and fabrication of living replacement devices for surgical reconstruction and transplantation. *Lancet.* 1999; 354(Suppl 1):SI32–4. [PubMed: 10437854]
7. Moutos FT, Freed LE, Guilak F. A biomimetic three-dimensional woven composite scaffold for functional tissue engineering of cartilage. *Nat Mater.* 2007; 6(2):162–7. [PubMed: 17237789]
8. Moutos FT, Guilak F. Functional properties of cell-seeded three-dimensionally woven poly(epsilon-caprolactone) scaffolds for cartilage tissue engineering. *Tissue Eng Part A.* 2010; 16(4):1291–301. [PubMed: 19903085]
9. Valonen PK, Moutos FT, Kusanagi A, Moretti MG, Diekman BO, Welter JF, et al. In vitro generation of mechanically functional cartilage grafts based on adult human stem cells and 3D-woven poly(epsilon-caprolactone) scaffolds. *Biomaterials.* 2010; 31(8):2193–200. [PubMed: 20034665]
10. Diekman BO, Guilak F. Stem cell-based therapies for osteoarthritis: challenges and opportunities. *Curr Opin Rheumatol.* 2013; 25(1):119–26. [PubMed: 23190869]
11. Jacques C, Gosset M, Berenbaum F, Gabay C. The role of IL-1 and IL-1Ra in joint inflammation and cartilage degradation. *Vitam Horm.* 2006; 74:371–403. [PubMed: 17027524]
12. Kapoor M, Martel-Pelletier J, Lajeunesse D, Pelletier JP, Fahmi H. Role of proinflammatory cytokines in the pathophysiology of osteoarthritis. *Nat Rev Rheumatol.* 2011; 7(1):33–42. [PubMed: 21119608]
13. Schlaak JF, Pfers I, Meyer Zum Buschenfelde KH, Marker-Hermann E. Different cytokine profiles in the synovial fluid of patients with osteoarthritis, rheumatoid arthritis and seronegative spondylarthropathies. *Clin Exp Rheumatol.* 1996; 14(2):155–62. [PubMed: 8737721]
14. Wilusz RE, Weinberg JB, Guilak F, McNulty AL. Inhibition of integrative repair of the meniscus following acute exposure to interleukin-1 in vitro. *J Orthop Res.* 2008; 26(4):504–12. [PubMed: 18050309]
15. McNulty AL, Moutos FT, Weinberg JB, Guilak F. Enhanced integrative repair of the porcine meniscus in vitro by inhibition of interleukin-1 or tumor necrosis factor alpha. *Arthritis Rheum.* 2007; 56(9):3033–42. [PubMed: 17729298]
16. Riera KM, Rothfus NE, Wilusz RE, Weinberg JB, Guilak F, McNulty AL. Interleukin-1, tumor necrosis factor-alpha, and transforming growth factor-beta 1 and integrative meniscal repair: influences on meniscal cell proliferation and migration. *Arthritis Res Ther.* 2011; 13(6):R187. [PubMed: 22087734]

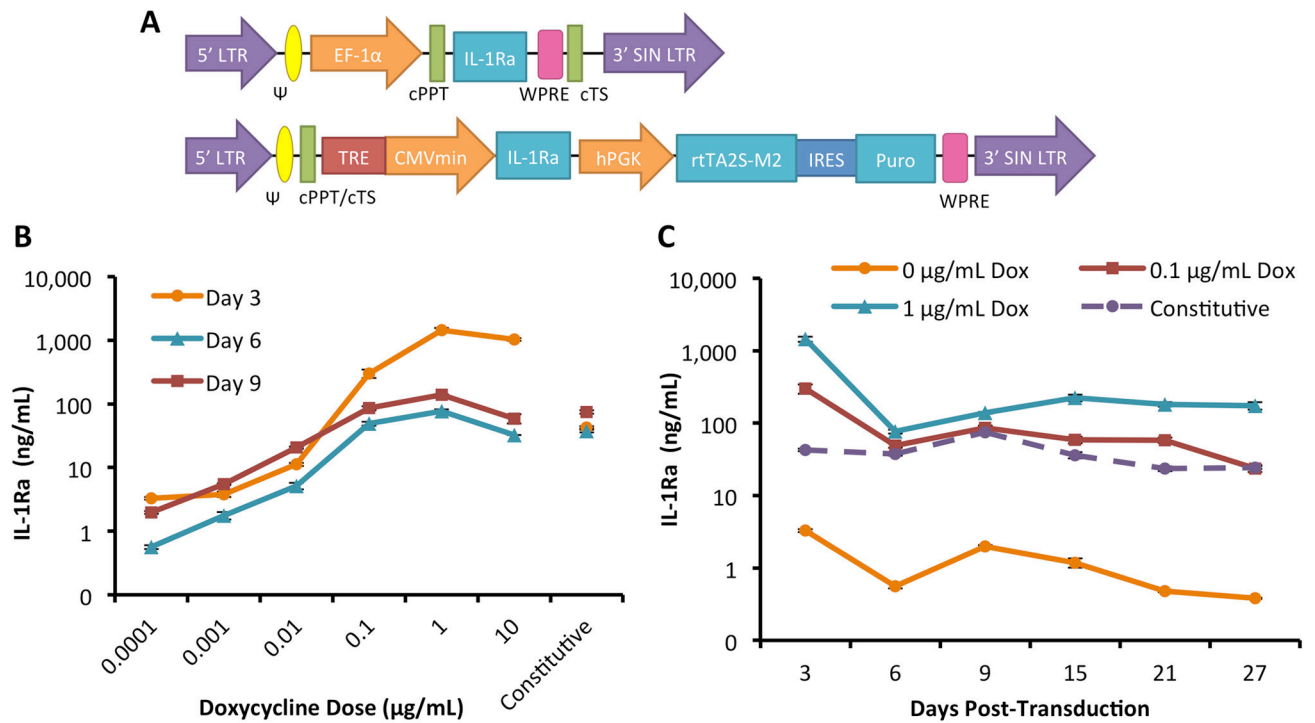


17. Heldens GT, Blaney Davidson EN, Vitters EL, Schreurs BW, Piek E, van den Berg WB, et al. Catabolic factors and osteoarthritis-conditioned medium inhibit chondrogenesis of human mesenchymal stem cells. *Tissue Eng Part A*. 2012; 18(1–2):45–54. [PubMed: 21770865]
18. Wehling N, Palmer GD, Pilapil C, Liu F, Wells JW, Muller PE, et al. Interleukin-1beta and tumor necrosis factor alpha inhibit chondrogenesis by human mesenchymal stem cells through NF-kappaB-dependent pathways. *Arthritis Rheum*. 2009; 60(3):801–12. [PubMed: 19248089]
19. Rainbow RS, Kwon H, Foote AT, Preda RC, Kaplan DL, Zeng L. Muscle cell-derived factors inhibit inflammatory stimuli-induced damage in hMSC-derived chondrocytes. *Osteoarthritis Cartilage*. 2013; 21(7):990–8. [PubMed: 23611899]
20. Ousema PH, Moutos FT, Estes BT, Caplan AI, Lennon DP, Guilak F, et al. The inhibition by interleukin 1 of MSC chondrogenesis and the development of biomechanical properties in biomimetic 3D woven PCL scaffolds. *Biomaterials*. 2012; 33(35):8967–74. [PubMed: 22999467]
21. Scotti C, Piccinini E, Takizawa H, Todorov A, Bourguine P, Papadimitropoulos A, et al. Engineering of a functional bone organ through endochondral ossification. *Proc Natl Acad Sci U S A*. 2013; 110(10):3997–4002. [PubMed: 23401508]
22. Farrell E, Both SK, Odorfer KI, Koevoet W, Kops N, O'Brien FJ, et al. In-vivo generation of bone via endochondral ossification by in-vitro chondrogenic priming of adult human and rat mesenchymal stem cells. *BMC Musculoskelet Disord*. 2011; 12:31. [PubMed: 21281488]
23. Ferreira E, Porter RM, Wehling N, O'Sullivan RP, Liu F, Boskey A, et al. Inflammatory cytokines induce a unique mineralizing phenotype in mesenchymal stem cells derived from human bone marrow. *J Biol Chem*. 2013; 288(41):29494–505. [PubMed: 23970554]
24. Mumme M, Scotti C, Papadimitropoulos A, Todorov A, Hoffmann W, Bocelli-Tyndall C, et al. Interleukin-1beta modulates endochondral ossification by human adult bone marrow stromal cells. *Eur Cell Mater*. 2012; 24:224–36. [PubMed: 23007908]
25. Seckinger P, Lowenthal JW, Williamson K, Dayer JM, MacDonald HR. A urine inhibitor of interleukin 1 activity that blocks ligand binding. *J Immunol*. 1987; 139(5):1546–9. [PubMed: 2957429]
26. Chevalier X, Goupille P, Beaulieu AD, Burch FX, Bensen WG, Conrozier T, et al. Intraarticular injection of anakinra in osteoarthritis of the knee: a multicenter, randomized, double-blind, placebo-controlled study. *Arthritis Rheum*. 2009; 61(3):344–52. [PubMed: 19248129]
27. Evans CH, Ghivizzani SC, Robbins PD. Arthritis gene therapy and its tortuous path into the clinic. *Transl Res*. 2013; 161(4):205–16. [PubMed: 23369825]
28. Gerstenfeld LC, Cullinane DM, Barnes GL, Graves DT, Einhorn TA. Fracture healing as a post-natal developmental process: molecular, spatial, and temporal aspects of its regulation. *J Cell Biochem*. 2003; 88(5):873–84. [PubMed: 12616527]
29. Mangiapani, D. ORS Abstract. 2012.
30. Barde I, Zanta-Boussif MA, Paisant S, Leboeuf M, Rameau P, Delenda C, et al. Efficient control of gene expression in the hematopoietic system using a single Tet-on inducible lentiviral vector. *Mol Ther*. 2006; 13(2):382–90. [PubMed: 16275162]
31. Urlinger S, Baron U, Thellmann M, Hasan MT, Bujard H, Hillen W. Exploring the sequence space for tetracycline-dependent transcriptional activators: novel mutations yield expanded range and sensitivity. *Proc Natl Acad Sci U S A*. 2000; 97(14):7963–8. [PubMed: 10859354]
32. Watson RS, Broome TA, Levings PP, Rice BL, Kay JD, Smith AD, et al. scAAV-mediated gene transfer of interleukin-1-receptor antagonist to synovium and articular cartilage in large mammalian joints. *Gene Ther*. 2013; 20(6):670–7. [PubMed: 23151520]
33. Goodrich LR, Phillips JN, McIlwraith CW, Foti SB, Grieger JC, Gray SJ, et al. Optimization of scAAV IL-1ra in vitro and in vivo to deliver high levels of therapeutic protein for treatment of osteoarthritis. *Mol Ther Nucleic Acids*. 2013; 2:e70. [PubMed: 23385523]
34. Kay JD, Gouze E, Oligino TJ, Gouze JN, Watson RS, Levings PP, et al. Intra-articular gene delivery and expression of interleukin-1Ra mediated by self-complementary adeno-associated virus. *J Gene Med*. 2009; 11(7):605–14. [PubMed: 19384892]
35. Madry H, Cucchiari M, Terwilliger EF, Trippel SB. Recombinant adeno-associated virus vectors efficiently and persistently transduce chondrocytes in normal and osteoarthritic human articular cartilage. *Hum Gene Ther*. 2003; 14(4):393–402. [PubMed: 12659680]

36. Cucchiaroni M, Madry H, Ma C, Thurn T, Zurakowski D, Menger MD, et al. Improved tissue repair in articular cartilage defects in vivo by rAAV-mediated overexpression of human fibroblast growth factor 2. *Mol Ther*. 2005; 12(2):229–38. [PubMed: 16043094]
37. Brunger JM, Huynh NPT, Guenther CM, Perez-Pinera P, Moutos FT, Sanchez-Adams J, et al. Scaffold-mediated lentiviral transduction for functional tissue engineering of cartilage. *Proc Natl Acad Sci U S A*. Feb 18, 2014 published ahead of print.
38. Gossen M, Freundlieb S, Bender G, Muller G, Hillen W, Bujard H. Transcriptional activation by tetracyclines in mammalian cells. *Science*. 1995; 268(5218):1766–9. [PubMed: 7792603]
39. Wiznerowicz M, Szulc J, Trono D. Tuning silence: conditional systems for RNA interference. *Nat Methods*. 2006; 3(9):682–8. [PubMed: 16929312]
40. Salmon P, Trono D. Production and titration of lentiviral vectors. *Curr Protoc Hum Genet*. 2007; Chapter 12(Unit 12 0)
41. Phillips JE, Burns KL, Le Doux JM, Guldborg RE, Garcia AJ. Engineering graded tissue interfaces. *Proc Natl Acad Sci U S A*. 2008; 105(34):12170–5. [PubMed: 18719120]
42. Gersbach CA, Coyer SR, Le Doux JM, Garcia AJ. Biomaterial-mediated retroviral gene transfer using self-assembled monolayers. *Biomaterials*. 2007; 28(34):5121–7. [PubMed: 17698189]
43. Mow VC, Kuei SC, Lai WM, Armstrong CG. Biphasic creep and stress relaxation of articular cartilage in compression? Theory and experiments. *J Biomech Eng*. 1980; 102(1):73–84. [PubMed: 7382457]
44. Farndale RW, Buttle DJ, Barrett AJ. Improved quantitation and discrimination of sulphated glycosaminoglycans by use of dimethylmethylene blue. *Biochim Biophys Acta*. 1986; 883(2):173–7. [PubMed: 3091074]
45. Reddy GK, Enwemeka CS. A simplified method for the analysis of hydroxyproline in biological tissues. *Clin Biochem*. 1996; 29(3):225–9. [PubMed: 8740508]
46. McNulty AL, Rothfusz NE, Leddy HA, Guilak F. Synovial fluid concentrations and relative potency of interleukin-1 alpha and beta in cartilage and meniscus degradation. *J Orthop Res*. 2013; 31(7):1039–45. [PubMed: 23483596]
47. Bouffi C, Bony C, Courties G, Jorgensen C, Noel D. IL-6-dependent PGE2 secretion by mesenchymal stem cells inhibits local inflammation in experimental arthritis. *PLoS One*. 2010; 5(12):e14247. [PubMed: 21151872]
48. Bernardo ME, Fibbe WE. Mesenchymal stromal cells: sensors and switchers of inflammation. *Cell Stem Cell*. 2013; 13(4):392–402. [PubMed: 24094322]
49. Egg D. Concentrations of prostaglandins D2, E2, F2 alpha, 6-keto-F1 alpha and thromboxane B2 in synovial fluid from patients with inflammatory joint disorders and osteoarthritis. *Z Rheumatol*. 1984; 43(2):89–96. [PubMed: 6730731]
50. Johnstone B, Hering TM, Caplan AI, Goldberg VM, Yoo JU. In vitro chondrogenesis of bone marrow-derived mesenchymal progenitor cells. *Exp Cell Res*. 1998; 238(1):265–72. [PubMed: 9457080]
51. Diekman BO, Rowland CR, Lennon DP, Caplan AI, Guilak F. Chondrogenesis of adult stem cells from adipose tissue and bone marrow: induction by growth factors and cartilage-derived matrix. *Tissue Eng Part A*. 2010; 16(2):523–33. [PubMed: 19715387]
52. Lima EG, Tan AR, Tai T, Bian L, Stoker AM, Ateshian GA, et al. Differences in interleukin-1 response between engineered and native cartilage. *Tissue Eng Part A*. 2008; 14(10):1721–30. [PubMed: 18611148]
53. Ramachandran M, Achan P, Salter DM, Bader DL, Chowdhury TT. Biomechanical signals and the C-type natriuretic peptide counteract catabolic activities induced by IL-1beta in chondrocyte/agarose constructs. *Arthritis Res Ther*. 2011; 13(5):R145. [PubMed: 21914170]
54. Athanasiou KA, Agarwal A, Dzida FJ. Comparative study of the intrinsic mechanical properties of the human acetabular and femoral head cartilage. *J Orthop Res*. 1994; 12(3):340–9. [PubMed: 8207587]
55. Mow VC, Guo XE. Mechano-electrochemical properties of articular cartilage: their inhomogeneities and anisotropies. *Annu Rev Biomed Eng*. 2002; 4:175–209. [PubMed: 12117756]

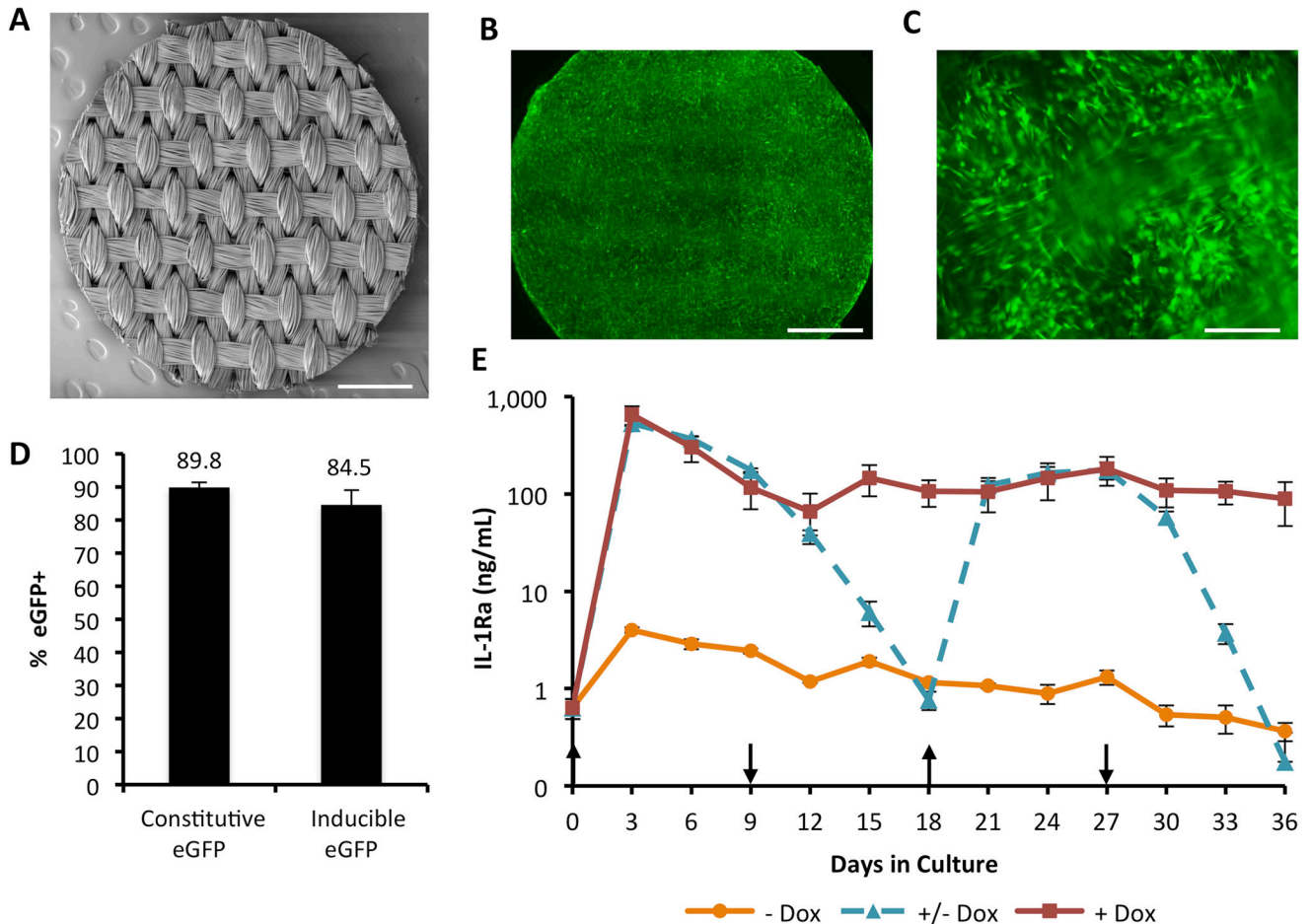
56. Mais A, Klein T, Ullrich V, Schudt C, Lauer G. Prostanoid pattern and iNOS expression during chondrogenic differentiation of human mesenchymal stem cells. *J Cell Biochem.* 2006; 98(4):798–809. [PubMed: 16440302]
57. Pountos I, Giannoudis PV, Jones E, English A, Churchman S, Field S, et al. NSAIDs inhibit in vitro MSC chondrogenesis but not osteogenesis: implications for mechanism of bone formation inhibition in man. *J Cell Mol Med.* 2011; 15(3):525–34. [PubMed: 20070439]
58. Goldring MB, Suen LF, Yamin R, Lai WF. Regulation of collagen gene expression by prostaglandins and interleukin-1beta in cultured chondrocytes and fibroblasts. *Am J Ther.* 1996; 3(1):9–16. [PubMed: 11856992]
59. Fermor B, Weinberg JB, Pisetsky DS, Misukonis MA, Fink C, Guilak F. Induction of cyclooxygenase-2 by mechanical stress through a nitric oxide-regulated pathway. *Osteoarthritis Cartilage.* 2002; 10(10):792–8. [PubMed: 12359165]
60. Clark CA, Schwarz EM, Zhang X, Ziran NM, Drissi H, O’Keefe RJ, et al. Differential regulation of EP receptor isoforms during chondrogenesis and chondrocyte maturation. *Biochem Biophys Res Commun.* 2005; 328(3):764–76. [PubMed: 15694412]
61. Nemeth K, Leelahavanichkul A, Yuen PS, Mayer B, Parmelee A, Doi K, et al. Bone marrow stromal cells attenuate sepsis via prostaglandin E(2)-dependent reprogramming of host macrophages to increase their interleukin-10 production. *Nat Med.* 2009; 15(1):42–9. [PubMed: 19098906]
62. Leddy HA, Awad HA, Guilak F. Molecular diffusion in tissue-engineered cartilage constructs: effects of scaffold material, time, and culture conditions. *J Biomed Mater Res B Appl Biomater.* 2004; 70(2):397–406. [PubMed: 15264325]
63. Shamji MF, Betre H, Kraus VB, Chen J, Chilkoti A, Pichika R, et al. Development and characterization of a fusion protein between thermally responsive elastin-like polypeptide and interleukin-1 receptor antagonist: sustained release of a local antiinflammatory therapeutic. *Arthritis Rheum.* 2007; 56(11):3650–61. [PubMed: 17968946]
64. Gorth DJ, Mauck RL, Chiaro JA, Mohanraj B, Hebel NM, Dodge GR, et al. IL-1ra delivered from poly(lactic-co-glycolic acid) microspheres attenuates IL-1beta-mediated degradation of nucleus pulposus in vitro. *Arthritis Res Ther.* 2012; 14(4):R179. [PubMed: 22863285]
65. Whitmire RE, Wilson DS, Singh A, Levenston ME, Murthy N, Garcia AJ. Self-assembling nanoparticles for intra-articular delivery of anti-inflammatory proteins. *Biomaterials.* 2012; 33(30):7665–75. [PubMed: 22818981]
66. Buhrmann C, Mobasheri A, Matis U, Shakibaei M. Curcumin mediated suppression of nuclear factor-kappaB promotes chondrogenic differentiation of mesenchymal stem cells in a high-density co-culture microenvironment. *Arthritis Res Ther.* 2010; 12(4):R127. [PubMed: 20594343]
67. Willard VP, Diekman BO, Sanchez-Adams J, et al. Osteoarthritis in a dish: the effects of pro-inflammatory cytokines on cartilage derived from induced pluripotent stem cells. *Osteoarthritis Cartilage.* 2013; 21(Supplement):S281–S2.
68. Hu WW, Wang Z, Hollister SJ, Krebsbach PH. Localized viral vector delivery to enhance in situ regenerative gene therapy. *Gene Ther.* 2007; 14(11):891–901. [PubMed: 17344901]
69. Gersbach CA, Phillips JE, Garcia AJ. Genetic engineering for skeletal regenerative medicine. *Annu Rev Biomed Eng.* 2007; 9:87–119. [PubMed: 17425467]
70. Basile P, Dadali T, Jacobson J, Hasslund S, Ulrich-Vinther M, Soballe K, et al. Freeze-dried tendon allografts as tissue-engineering scaffolds for Gdf5 gene delivery. *Mol Ther.* 2008; 16(3):466–73. [PubMed: 18180771]
71. Liao IC, Chen S, Liu JB, Leong KW. Sustained viral gene delivery through core-shell fibers. *J Control Release.* 2009; 139(1):48–55. [PubMed: 19539680]
72. Holladay C, Power K, Sefton M, O’Brien T, Gallagher WM, Pandit A. Functionalized scaffold-mediated interleukin 10 gene delivery significantly improves survival rates of stem cells in vivo. *Mol Ther.* 2011; 19(5):969–78. [PubMed: 21266957]
73. Shea LD, Smiley E, Bonadio J, Mooney DJ. DNA delivery from polymer matrices for tissue engineering. *Nat Biotechnol.* 1999; 17(6):551–4. [PubMed: 10385318]

74. Neumann AJ, Schroeder J, Alini M, Archer CW, Stoddart MJ. Enhanced adenovirus transduction of hMSCs using 3D hydrogel cell carriers. *Mol Biotechnol.* 2013; 53(2):207–16. [PubMed: 22382454]
75. Lee HH, O'Malley MJ, Friel NA, Chu CR. Effects of doxycycline on mesenchymal stem cell chondrogenesis and cartilage repair. *Osteoarthritis Cartilage.* 2013; 21(2):385–93. [PubMed: 23186943]
76. Brandt KD, Mazzuca SA, Katz BP, Lane KA, Buckwalter KA, Yocum DE, et al. Effects of doxycycline on progression of osteoarthritis: results of a randomized, placebo-controlled, double-blind trial. *Arthritis Rheum.* 2005; 52(7):2015–25. [PubMed: 15986343]



**Figure 1.**

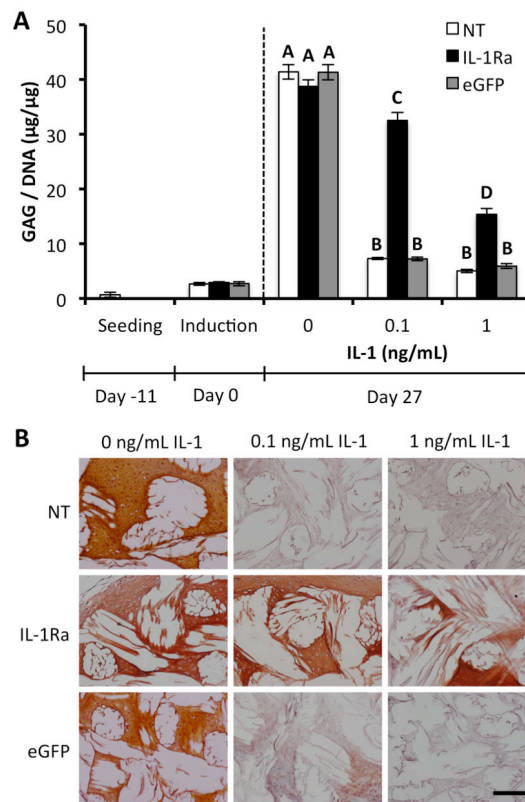
Tunable IL-1Ra expression in MSCs with a dox-inducible lentiviral vector. **A.** Schematic diagram of lentiviral vectors with IL-1Ra as the representative gene of interest. On top is the constitutive expression system driven by the elongation factor 1 alpha (EF-1 $\alpha$ ) promoter. Shown on bottom is the dox-inducible expression system. IL-1Ra is driven by the tetracycline-regulated minimal CMV promoter (TRE-CMVmin). The human phosphoglycerate kinase (hPGK) promoter constitutively drives expression of the tet-responsive transactivator (rtTA2S-M2) and then, following an internal ribosomal entry site (IRES), the puromycin resistance gene (puro) which enables selection of transduced cells. Both vectors contain the 5' and 3' long-terminal repeats (LTR), psi packaging signal ( $\Psi$ ), the central polypurine tract (cPPT), central termination sequence (cTS), and the woodchuck hepatitis virus post-transcriptional regulatory element (WPRE). **B.** IL-1Ra secretion tuned by dox dose from MSCs in monolayer culture. Shown is IL-1Ra secreted over 72 hours into culture medium on days 3, 6, and 9 following transduction (mean  $\pm$  SEM, n=3). **C.** IL-1Ra secretion from 3 to 27 days in monolayer culture at 3 dox doses or with constitutive expression. Shown is IL-1Ra secreted over 72 hours into culture medium (mean  $\pm$  SEM, n=3).



**Figure 2.**

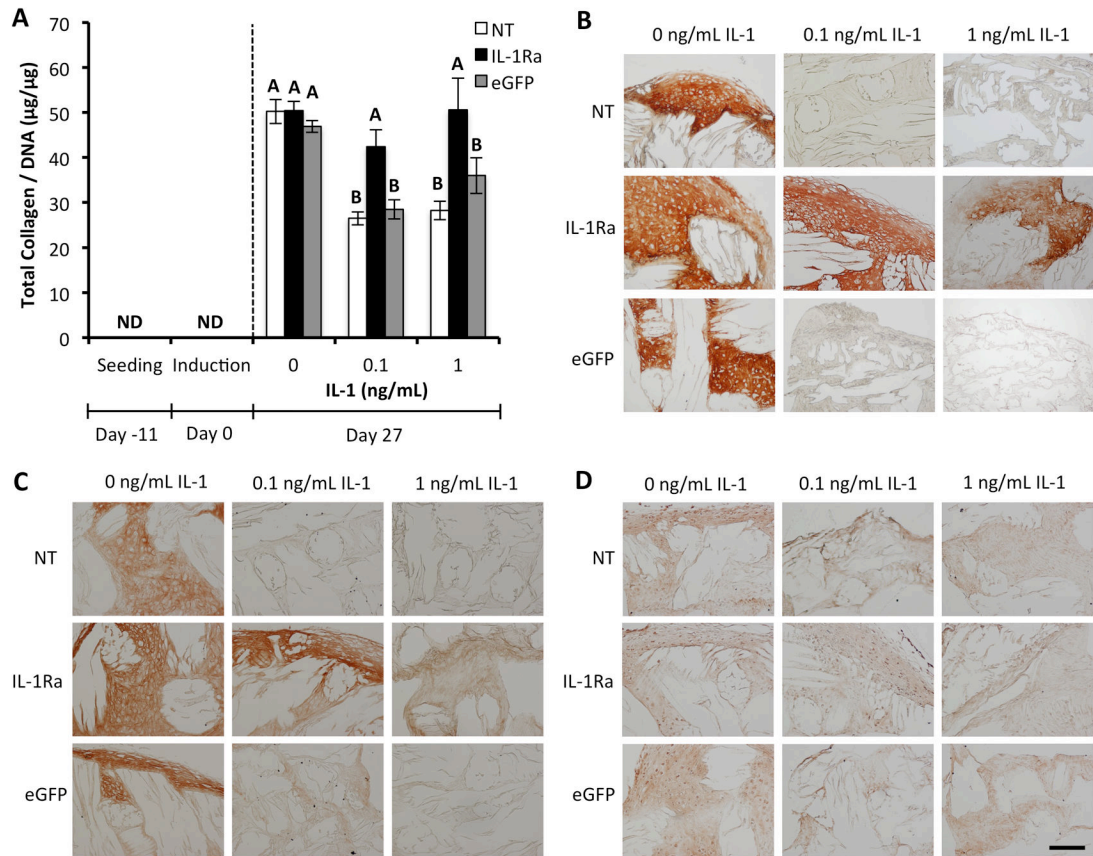
Scaffold-mediated LV transduction of MSCs within 3D woven PCL scaffolds. **A.** Scanning electron microscopy (SEM) image of a 3D woven PCL scaffold 5 mm disk. Scale bar = 1mm. **B.** Fluorescence image of constitutive eGFP-expressing MSCs on the 3D woven PCL scaffold 6 days after seeding. Scale bar = 1 mm, 300 ms exposure. **C.** Fluorescence image of constitutive eGFP-expressing MSCs on the 3D woven PCL scaffold 6 days after seeding. Scale bar = 250  $\mu$ m, 90 ms exposure. **D.** Scaffold-mediated transduction efficiency of MSCs with either constitutive or inducible eGFP-LV. MSCs were isolated from constructs at day 6 and the percentage of eGFP+ cells was measured via flow cytometry (mean  $\pm$  SEM, n=3, all samples given 1  $\mu$ g/mL dox). **E.** IL-1Ra secretion from engineered cartilage constructs into media every 72 hours over 36 days of chondrogenesis (mean  $\pm$  SEM, n=3). + **Dox** indicates dox induction at 1  $\mu$ g/mL for 36 days. - **Dox** indicates the baseline IL-1Ra expression in the absence of dox. +/- **Dox** indicates that dox (1  $\mu$ g/mL) was switched on and off every 9 days. Upward arrows show time points at which dox was induced and downward arrows show the withdrawal of dox.





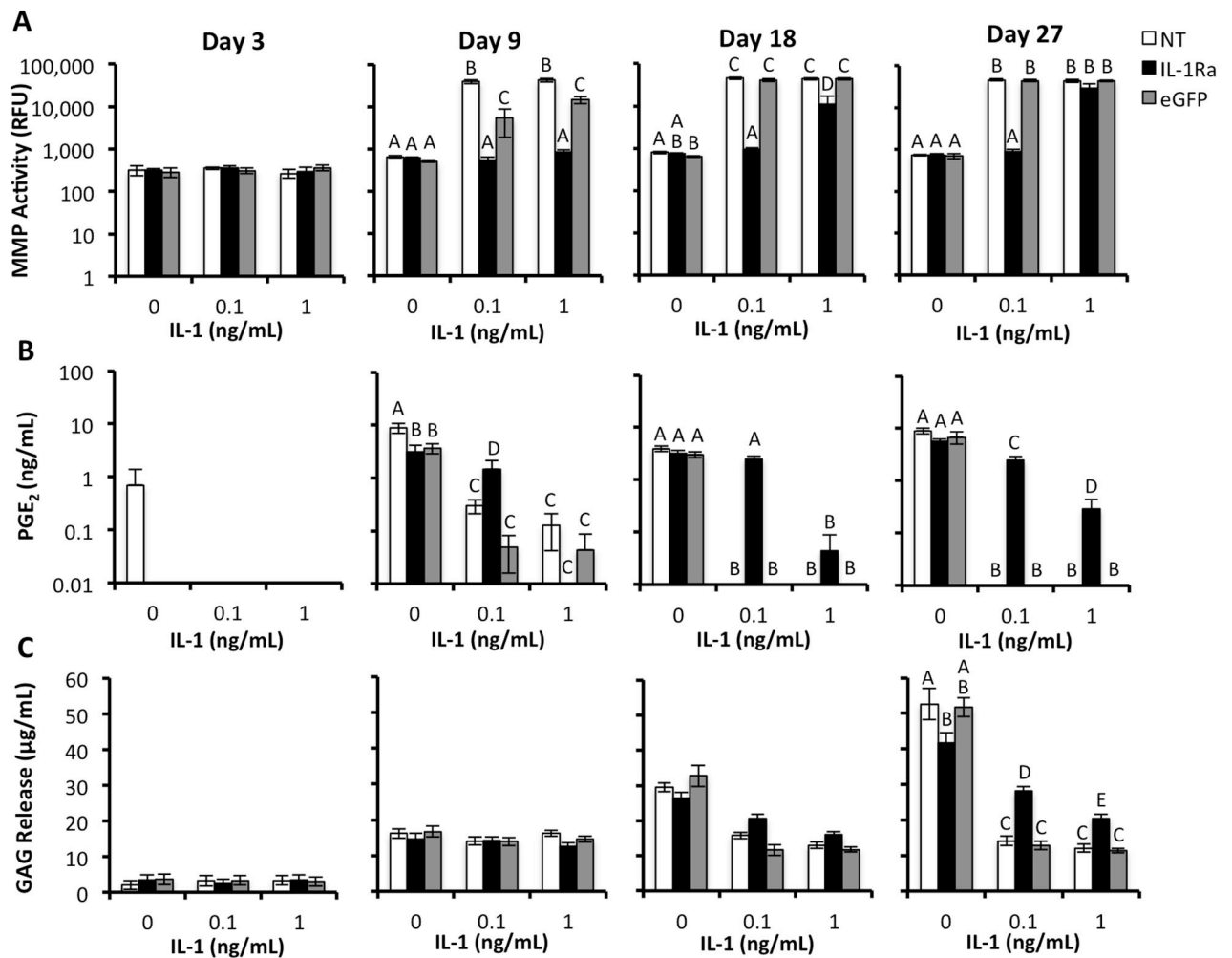
**Figure 3.**

IL-1Ra-expressing constructs maintain GAG content with IL-1 treatment. **A.** GAG per DNA content in engineered cartilage constructs at seeding, chondrogenic induction, and after 27 days of culture in chondrogenic media with either 0, 0.1, or 1 ng/mL IL-1 (mean  $\pm$  SEM,  $n=5$ ). NT indicates non-transduced constructs. IL-1Ra indicates constructs transduced with IL-1Ra LV. eGFP indicates constructs transduced with eGFP LV. Groups with different letters are significantly different ( $P<0.05$ ) by ANOVA and Fisher's LSD post-hoc. **B.** Safranin-O red and fast green staining for GAGs and collagen, respectively. The white space shows the location of the PCL fiber bundles. All sections 8  $\mu\text{m}$ . Scale bar = 200  $\mu\text{m}$ .



**Figure 4.**

IL-1Ra-expressing constructs maintain collagen content with IL-1 treatment. **A.** Collagen per DNA content in engineered cartilage constructs at seeding, chondrogenic induction, and after 27 days of culture in chondrogenic media with either 0, 0.1, or 1 ng/mL IL-1 (mean  $\pm$  SEM, n=5). NT indicates non-transduced constructs. IL-1Ra indicates constructs transduced with IL-1Ra LV. eGFP indicates constructs transduced with eGFP LV. Groups with different letters are significantly different ( $P < 0.05$ ) by ANOVA and Fisher's LSD post-hoc. ND = nondetectable. Immunohistochemistry staining for **B.** Type II collagen. **C.** Type I collagen. **D.** Type X collagen. All sections 8  $\mu$ m. Scale bar = 200  $\mu$ m.

**Figure 5.**

Analyses of inflammatory mediators and ECM released into culture media by engineered cartilage constructs during chondrogenesis (days 3,9,18,27) and treatment with either 0, 0.1, or 1 ng/mL IL-1. NT indicates non-transduced constructs. IL-1Ra indicates constructs transduced with IL-1Ra LV. eGFP indicates constructs transduced with eGFP LV. For all analyses, groups with different letters are significantly different ( $P < 0.05$ ) by ANOVA and Fisher's LSD post-hoc (mean  $\pm$  SEM,  $n=5$ ). **A.** Total specific activity of MMPs released into culture media. **B.** Concentration of PGE<sub>2</sub> released into culture media. **c.** Concentration of GAG released into culture media.

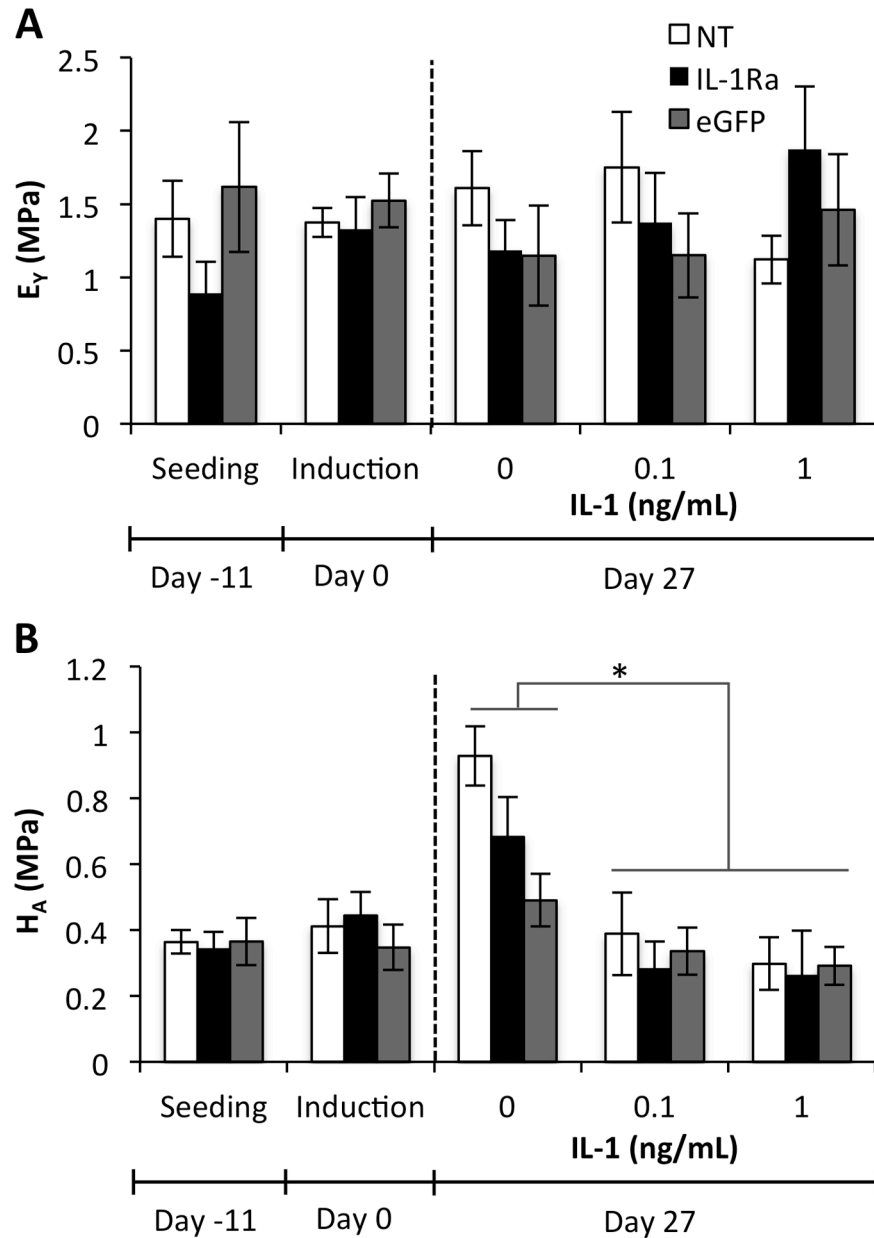


**Figure 6.** Mechanical properties of engineered cartilage constructs at seeding, chondrogenic induction, and after 27 days of culture in chondrogenic media with either 0, 0.1, or 1 ng/mL IL-1 (mean  $\pm$  SEM, n=5). NT indicates non-transduced constructs. IL-1Ra indicates constructs transduced with IL-1Ra LV. eGFP indicates constructs transduced with eGFP LV. **A.** Equilibrium Young's modulus ( $E_Y$ ). No significant interaction or main effects were found by ANOVA. **B.** Aggregate modulus ( $H_A$ ). IL-1 treatment was significantly different than no IL-1 treatment at Day 27 ( $p < 0.05$ ), but no significant interaction or main effect of vector was observed by ANOVA.